ESR and optical absorption spectra of reduced vanadium ions in Ca2NaMg2V3O12 garnet

Oversluizen, G.; Metselaar, R.

ESR and optical absorption spectra of reduced vanadium ions in $Ca_2NaMg_2V_3O_{12}$ garnet

G Oversluizen and R Metselaar

Laboratory of Physical Chemistry, Eindhoven University of Technology, Eindhoven, The Netherlands

Abstract. Optical absorption and ESR spectra of reduced vanadium centres in $Ca_2NaMg_2V_3O_{12}$ are reported. The spectra are interpreted as arising from tetrahedrally coordinated V^{4+} and octahedrally coordinated V^{3+}. The ESR and optical data are correlated using molecular orbital (MO) theory. The composition of the flux-grown single crystals is analysed and discussed.

1. Introduction

The garnets form a class of compounds that crystallise in the cubic system with space-group O_h^{10} ($Ia3d$). There are three kinds of cation sites all of which are usually occupied. The general formula is $\{C_3\}[A_2](D_3)O_{12}$, in which $\{C\}$ denotes ions on dodecahedral sites, [A] ions on octahedral sites and (D) ions on tetrahedral sites. The iron garnets, such as $\{Y_3\}[Fe_2](Fe_3)O_{12}$, have attracted especially great attention due to their interesting ferrimagnetic properties. Light-induced changes in physical properties have also been studied widely. Studies of the effect of electron donating centres, created by doping or partial reduction, have been helpful for the understanding of these light-induced effects (Metselaar 1977, Metselaar and Larsen 1978). However, the presence of transition-metal ions in two or three sublattices forms an extra complication, especially in the understanding of the charge-transport mechanism and photoconductivity results (Metselaar and Larsen 1978, Suryanarayanan and Krishnan 1974). For this reason we have started a study of garnets in which transition-metal ions are only found in one sublattice.

In this paper results of optical and ESR measurements on $\{Ca_2Na\}[Mg_2](V_3)O_{12}$ are presented. In the iron garnets many of the interesting physical properties are due to the presence of small amounts of Fe^{2+} ions in the Fe^{3+} sublattices. The vanadate garnet was chosen because it is known that small concentrations of V^{4+} ions can be present in the V^{5+} sublattice (Havlicek *et al* 1971). Contrary to the case of Fe^{2+} in the ferrimagnetic iron garnets, the properties of the isolated V^{4+} ion can be easily studied, due to its paramagnetic properties. In § 2 the preparation of single crystals is described, together with the characterisation by means of electron microprobe, x-ray analysis and weight-loss measurements, and § 3 gives experimental details. In §§ 4 and 5 optical absorption

spectra and ESR results are presented and discussed. The results are compared and discussed in relation to the literature data in § 6, and the conclusions drawn are summarised in § 7.

2. Preparation and characterisation

Polycrystalline $Ca_2NaMg_2V_3O_{12}$ has been prepared by solid state reaction following a synthesis first described by Durif (1958). The component oxides and carbonates, Na_2CO_3, $CaCO_3$ and MgO, V_2O_5, were of at least p.a. purity grade. Weighed stoichiometric quantities were mixed by conventional ball-milling in agate mortars and fired in air at 700 °C for 10 h. Single crystals have been grown from V_2O_5 and PbO fluxes with molar compositions $1Ca_2NaMg_2V_3O_{12} + 1.5V_2O_5$, $1Ca_2NaMg_2V_3O_{12} + 1.2V_2O_5$ and $1Ca_2NaMg_2V_3O_{12} + 1.2PbO$, respectively. Tightly covered platinum crucibles containing about 30 cm^3 of the melt were placed in the centre of a resistance furnace and heated to 1200 °C in 6 h. The furnace was cooled at 2 °C h^{-1} from 1200 °C to 800 °C where the power was turned off. The resulting crystals were separated from the flux by leaching in hot NH_4OH. The greater part of the crystals had some well developed faces. Crystal dimensions were typically of the order 1–2 mm and in individual cases 4–5 mm. Further reduction of the cooling rate did not increase the crystal dimensions. Similar synthesis have been described in the literature (Ronniger *et al* 1974). All diffraction lines present in the recorded x-ray patterns could be indexed in the $Ia3d$ space group.

The lattice parameters were accurately determined from Guinier pictures using Al_2O_3 as the internal standard. The compositions of the single crystals were evaluated relative to the polycrystalline material by x-ray analysis on a Jeol 733 electron microprobe. The lead content was calculated with respect to a PbO standard. Lead is known to be readily incorporated in garnets of this type (Ronniger and Mill 1973).

A method based on buoyancy was used to determine the crystal density (Prokic 1974). Several characteristics of the prepared garnets are summarised in table 1. Thermogravimetric experiments performed in air indicated an irreversible weight loss starting at approximately 900 °C and continuing at a rate of about 3×10^{-4} wt% h^{-1} at 1100 °C. This weight loss was accompanied by an increase of the lattice parameter and a reduced content of ions—mainly Ca, Na and Mg ions. Long heating periods at temperatures above 1050 °C resulted in the formation of an unidentified second phase. In this two-phase material the lattice parameter of the garnet remained constant at 12.439 Å.

Near 1100 °C a reversible reduction reaction occured simultaneously, producing V^{4+} centres. In the single crystals V^{4+} centres were produced by a heat treatment for 15 min at 1120–1140 °C in air, followed by an air quench to room temperature. Similar results can be obtained in polycrystalline sintered pellets; however, polycrystalline powdered samples reoxidise during quenching.

All measurements reported in this paper were performed on homogeneous single-phase crystals as verified by optical microscopy, scanning microscopy and electron microprobe measurements.

3. Experimental details

Thin plane parallel plates of 0.5–1 mm thickness were prepared from the crystals by grinding and polishing with diamond discs. Room-temperature optical absorption spec-

Table 1. Physical constants and growth characteristics of $Ca_2NaMg_2V_3O_{12}$.

Composition	Lattice parameter (± 0.001 Å)	x-ray density (g cm^{-3})	Experimental density (g cm^{-3})	Colour	Facetting
$Ca_2NaMg_2V_3O_{12}$	12.435	3.431		White powder	
$Ca_{2.05}Na_{0.60}Mg_{2.11}V_{2.99}O_{12}$	12.423	3.406	3.40	Reddish single crystal	{211} > {110}
$Ca_{1.94}Na_{0.91}Pb_{0.10}Mg_{1.92}V_{2.99}O_{12}$	12.453	3.511	3.52	Transparent single crystal	{211} > {110}

Table 2. Parameters of the axial spin Hamiltonian as deduced from the ESR spectra at 77 K.

Composition	$g_\parallel$	$g_\perp$	$|A_\parallel|(10^{-4}$ cm$^{-1})$	$|A_\perp|(10^{-4}$ cm$^{-1})$
$Ca_{2.05}Na_{0.60}Mg_{2.11}V_{2.99}O_{12}$	1.8569 ± 0.0004	1.9801 ± 0.0005	152.8 ± 0.3	31.9 ± 0.3
$Ca_{1.94}Na_{0.91}Pb_{0.10}Mg_{1.92}V_{2.99}O_{12}$	1.8549 ± 0.0003	1.9785 ± 0.0003	150.1 ± 0.2	31.0 ± 0.2
Nominal $Ca_2NaMg_2V_3O_{12}$[a]	1.856 ± 0.002	1.979 ± 0.001	152	31

[a] Havlicek *et al* (1971).
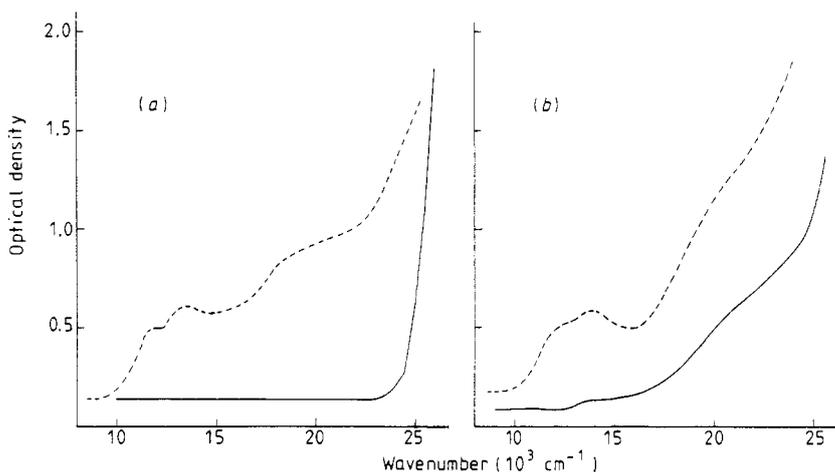
Figure 1. Absorption spectrum at room temperature of (a) $Ca_{1.94}Na_{0.91}Pb_{0.10}Mg_{1.92}V_{2.99}O_{12}$, sample thickness 1.7 mm, and (b) $Ca_{2.05}Na_{0.60}Mg_{2.11}V_{2.99}O_{12}$, sample thickness 1.0 mm: ——as grown; - - - - - after heat treatment.

tra were measured with a Zeiss PMQ II spectrometer. ESR spectra were recorded on a Varian E-15 spectrometer operating at X-band frequencies with 100 kHz RF modulation. The magnetic fields were measured with an NMR probe to within 0.1 G and the frequency was monitored using a Hewlett–Packard model 2590 B transfer oscillator and a model 5245 L electronic counter. The samples were placed in the centre of a T102 cavity equipped with a liquid helium continuous-flow cryostat (Oxford Instruments). The temperature was controlled to within 0.5 K by means of a Cryoson VC30 temperature controller.

Preliminary crystallographic orientation of the single crystals was performed by the x-ray Laue back-reflection technique. Then the crystals were glued to a holder with the (100) or (110) planes perpendicular to the axis of rotation. Final orientation was carried out, according to the extreme value of the magnetic resonance field of the low-field lines.

4. Results

4.1. Optical absorption

Absorption spectra recorded before and after heat treatment of the crystals are shown in figure 1.

The garnet as grown from the PbO flux is transparent up to a strong absorption edge situated at $25\,500$ cm^{-1}. After the heat treatment a double absorption band in the infrared, with maxima at 11900 and 13500 cm^{-1}, is seen, together with an increased absorption in the $(16-25) \times 10^3$ cm^{-1} region. The absorption spectra of crystals grown from a V_2O_5 flux show essentially the same features, apart from the weakly structured absorption responsible for the reddish colour of the untreated crystals. Tentatively this absorption may be decomposed into two bands at 14000 and 22000 cm^{-1}. An attempt to obtain a better resolution at liquid nitrogen temperature was not successful. In crystals grown from a V_2O_5 flux the double band in the near infrared is shifted to slightly higher energies as compared with that of crystals grown from a PbO flux.
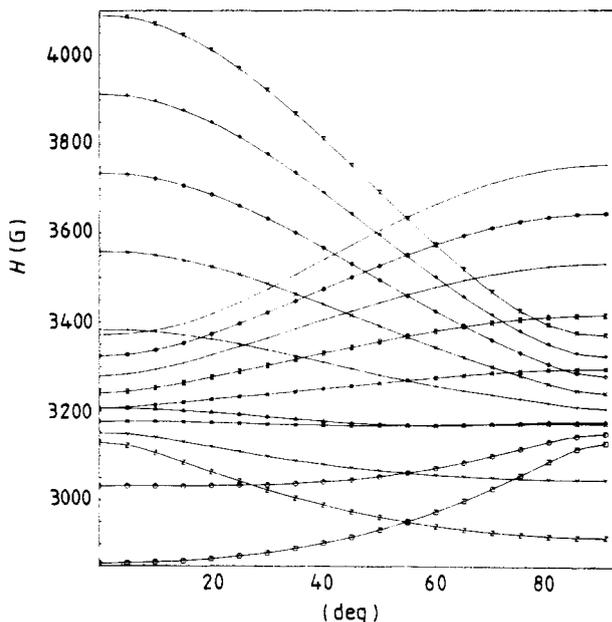
Figure 2. Angular dependence of ESR lines when the field is rotated in the (110) plane; 0°, $H \parallel [001]$, 90°, $H \parallel [110]$. Microwave frequency 9.0285 GHz.

4.2. Electron spin resonance

In the untreated crystals no ESR signal could be detected in the available field range $0{-}10^4$ G, even at 4.2 K. After heat treatment the response of an $S = \frac{1}{2}$ centre was detected, with a characteristic hyperfine splitting due to an $I = \frac{7}{2}$ isotope.

No change of resonance positions was observed with temperature. Above 77 K the lines broaden, probably due to spin–lattice relaxation. Below 77 K saturation becomes important and at 4.2 K unsaturated signals were only obtained at minimum klystron power.

Figure 2 shows the angular dependence at 77 K when the magnetic field (H) is rotated in a (110) plane. Evidently the spectra exhibit tetragonal local symmetry with the distortion axis coinciding with one of the cubic axes. Assuming coinciding principle axes of the g and A (hyperfine) tensors and neglecting nuclear quadrupole interactions the appropriate spin Hamiltonian is

$$\mathcal{H} = \beta[g_\parallel H_z S_z + g_\perp (H_x S_x + H_y S_y)] + A_\parallel I_z S_z + A_\perp (I_x S_x + I_y S_y). \tag{1}$$

An accurate fit with the experimental angular variation was obtained by considering the hyperfine interaction up to second order (Abragam and Bleaney 1970). The calculated spin Hamiltonian parameters are given in table 2. For comparison, data previously reported by Havlicek *et al* (1971) have been included in this table.

5. Interpretation of the spectra

5.1. Tetrahedral V^{4+}

The V^{5+} isotope with nuclear spin $I = \frac{7}{2}$ has a natural abundance of 99.76%. Further it is known that the tetrahedral sites in garnets are distorted along the cubic axis with site

symmetry S_4 (Geller 1967). One therefore readily attributes the observed ESR spectrum to V^{4+} ions on tetrahedral sites.

The splitting of ^2D states in an axial field is shown in figure 3. The ground state can be inferred from the relative magnitude of the spin Hamiltonian parameters. Crystal-field theory predicts $g_\parallel < g_\perp$ if the tetrahedron is elongated and $g_\perp < g_\parallel$ if the tetrahedron is compressed (Wertz and Bolton 1972). By comparing these expressions with the experimental values, it is seen that the tetrahedron is elongated, corresponding to a $d_{x^2-y^2}$ ground state. This agrees with the results of crystallographic structure refinements in similar garnets (Dukhovskaya and Mill 1974). As the ESR V^{4+} signal and the double band in the optical absorption spectra appear and disappear simultaneously with reduction and reoxidation of the samples respectively, it seems natural to ascribe these features to the same centre. The observed $\simeq 12000$ and $\simeq 13500$ cm^{-1} absorptions are then assigned to transitions from the $^2B_1$ ground state to the $^2B_2$ and ^2E levels. This assignment requires a crystal-field parameter $10\,Dq \simeq 12500$ cm^{-1} and a tetragonal-field splitting of $\simeq 1500$ cm^{-1}. The above values are in general agreement with those reported by Weber and Riseberg (1971) for reduced vanadium centres in YAG, as shown in table 3. The ESR and optical absorption data can be correlated using molecular orbital (MO) theory.

Table 3. Transition energies of reduced vanadium centres in YAG (Weber and Riseberg 1971).

Centre	Transition energy (10^3 cm^{-1})	Assignment
V^{4+} tetrahedral	12.5	$^2E \rightarrow {}^2T_2$
	14.4	
V^{4+} octahedral	20.2	$^2T_2 \rightarrow {}^2E$
	23.0	
V^{3+} tetrahedral	8.0	$^3A_2 \rightarrow {}^3T_2$
V^{3+} octahedral	16.3	$^3T_1 \rightarrow {}^3T_2$
	23.5	$^3T_1 \rightarrow {}^3T_1$

Neglecting the usually small corrections due to overlap integrals, the spin Hamiltonian parameters may be expressed as (Kivelson and Neiman 1961)

$$g_\parallel = g_e - 8\lambda_0 B_{x^2-y^2}^2 B_{xy}^2/\Delta_\parallel$$

$$g_\perp = g_e - 2\lambda_0 B_{x^2-y^2}^2 B_{xz,yz}^2/\Delta_\perp \tag{2}$$

$$A_\parallel = -P[(\tfrac{4}{7} + \kappa)B_{x^2-y^2}^2 - (g_\parallel - g_e) - \tfrac{3}{7}(g_\perp - g_e)]$$

$$A_\perp = -P[(\kappa - \tfrac{2}{7})B_{x^2-y^2}^2 - \tfrac{11}{14}(g_\perp - g_e)] \tag{3}$$

where $B_{x^2-y^2}$, B_{xy}, $B_{xz,yz}$ are the fractions of d-like orbital in the corresponding anti-bonding functions, $g_e = 2.0023$ is the free-electron spin g-factor, $\lambda_0 = 248$ cm^{-1} is the free-ion spin–orbit coupling constant (Fraga *et al* 1976), $\Delta_\parallel$ and $\Delta_\perp$ are the optical transition energies indicated in figure 3, κ is a term representing the Fermi contact interaction and P is related to the average value of r^{-3} for the free ion by

$$P = (2\beta_e\mu_N/I) \langle r^{-3} \rangle. \tag{4}$$

Taking $\mu_N = 5.14\beta_N$ (Abragam and Bleaney 1970), $I = \tfrac{7}{2}$ and $\langle r^{-3} \rangle = 3.67$ au (Fraga *et al* 1976), a theoretical estimate $P = 172 \times 10^{-4}$ cm^{-1} is obtained. Insertion of this value in the hyperfine equations (3) yields either $B_{x^2-y^2} \simeq 0.66$, with B_{xy} and B_{xz} as determined

from equations (2), close to one, or $B_{x^2-y^2} > 1$ for the two respective sign choices possible: $A_\parallel < 0, A_\perp < 0$ and $A_\parallel < 0, A_\perp > 0$. Such values are physically unrealistic as argued below. Therefore V^{4+} ESR data were gathered from the literature to obtain an experimental estimate of P (table 4).

Elimination of κ from the hyperfine equations (3) yields

$$A_\parallel - A_\perp = -P[\tfrac{6}{7}B^2_{x^2-y^2} - (g_\parallel - g_e) + \tfrac{3}{14}(g_\perp - g_e)]. \tag{5}$$

In what follows the MO coefficient of the ground-state orbital appearing in equation (5) will be referred to as B because in the distorted octahedral sites also considered in table 4 the ground state corresponds to a d_{xy} orbital.

For Δg values of the order 0.1, the product PB^2 is rather insensitive to the exact value chosen for B. The fact that P is expected to be positive reduces the sign possibilities to $A_\parallel < 0, A_\perp < 0$ and $A_\parallel < 0, A_\perp > 0$. The calculated PB^2 values, assuming $B = 1$, for a number of tetragonal V^{4+} centres in different compounds are listed in table 4.

From the table we observe a striking correspondence between PB^2 values for V^{4+} in different compounds if it is assumed that $A_\parallel$ and $A_\perp$ are both negative. On the other hand the assumptions $A_\parallel < 0, A_\perp > 0$ lead to widely varying values of PB^2. If the maximum value of PB^2 is considered to correspond to complete ionicity in the ground state, that is $P = 122 \times 10^{-4} \, \mathrm{cm}^{-1}$, a recalculation of the MO coefficients yields $0.92 < B < 1.0$. Values close to one should indeed be expected because the selection of the ground state is essentially the result of the small interaction of the orbital concerned with the surroundings (McClure 1959). MO coefficients, obtained using $P = 122 \times 10^{-4} \, \mathrm{cm}^{-1}$, band data and assignments are summarised in table 5.

The difference in transition energies between the two compounds clearly demonstrates the reduction of the crystal field on enlargement of the lattice parameter (compare table 1), whilst a marked difference between MO coefficients is not observed. Although the accuracy of the MO coefficients is limited by the inaccuracy of all other parameters
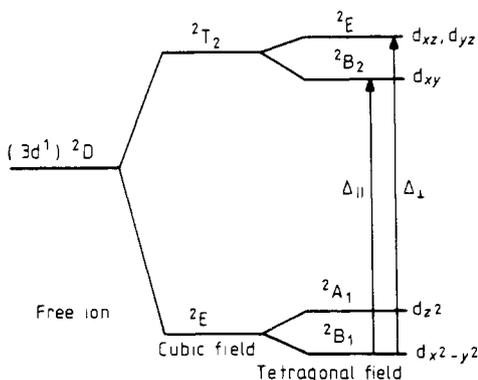

Figure 3. Energy level scheme of V^{4+} ($3d^1$) ions on a tetrahedral site with tetragonal deformation.
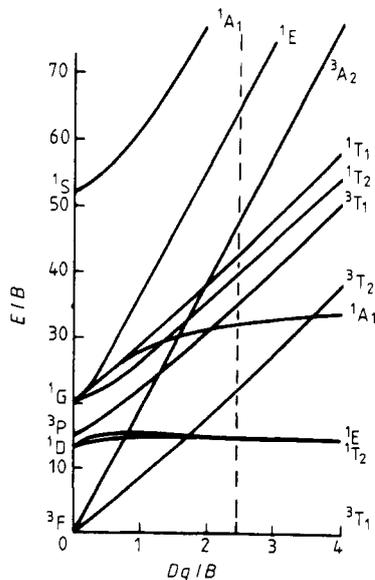

Figure 4. Energy levels of V^{3+} ($3d^2$) in an octahedral crystal field. The best fit with the experimental results is marked by a broken line.

Table 4. Calculated values of PB^2.

Host	Reference	$g_\parallel$	$g_\perp$	$\|A_\parallel\|$ (10^{-4} cm^{-1})	$\|A_\perp\|$ (10^{-4} cm^{-1})	PB^2 (10^{-4} cm^{-1})	
						$B=1, A_\perp<0$	$B=1, A_\perp>0$
AlPO$_4$	a	1.9168	1.9835	188	75	121	281
ZnCs$_2$(SO$_4$)$_2$·6H$_2$O	b	1.935	1.986	182	73	119	178
MAG alum	c	1.939	1.976	174.2	67	118	165
GeO$_2$ (amorphous)	d	1.929	1.976	175.5	68.2	117	165
GeO$_2$	d	1.963	1.921	134	37	112	197
TiO$_2$	e	1.956	1.914	142	37	121	207
SrTiO$_2$	f	1.9420	1.8945	146.8	44.0	117	218
Ca$_{2.05}$Na$_{0.60}$Mg$_{2.11}$V$_{2.99}$O$_{12}$	g	1.8569	1.9801	152.8	31.9	122	186
Ca$_{1.94}$Na$_{0.91}$Pb$_{0.10}$Mg$_{1.92}$V$_{2.99}$O$_{12}$	g	1.8549	1.9785	150.1	31.0	120	182

[a] De Biasi (1980). [b] Jain and Srinivasan (1977). [c] Raq et al (1969). [d] Siegel (1964). [e] Gerritsen and Lewis (1960). [f] Kool and Glaskeek (1979). [g] This work.

Table 5. MO coefficients, band data, assignments and crystal-field parameters.

Compound	Optical transition energy (10^3 cm^{-1})	Assignments	Crystal-field parameters (cm^{-1})		$B_{x^2-y^2}$	B_{xy}	B_{xz}	κ
			cubic	tetragonal				
Ca$_{2.05}$Na$_{0.60}$Mg$_{2.11}$V$_{2.99}$O$_{12}$	12.4	$^2B_1 \rightarrow {}^2B_2$	12200	1500	1.00	0.95	0.79	0.53
	13.9	$^2B_1 \rightarrow {}^2E$						
Ca$_{1.94}$Na$_{0.91}$Pb$_{0.10}$Mg$_{1.92}$V$_{2.99}$O$_{12}$	11.9	$^2B_1 \rightarrow {}^2B_2$	11700	1500	0.99	0.95	0.81	0.51
	13.4	$^2B_1 \rightarrow {}^2E$						

involved in their determination, the above observation is felt to be indicative of the dimensional insensibility of MO coefficients. However, the main conclusions to be drawn from these results are: (i) the assumption that the V^{4+} ion is situated at the tetrahedral sublattice is correct; (ii) the Fermi contact interaction contributes significantly to the hyperfine coupling parameters; (iii) the ground state may be regarded as ionic whereas the ^{2}E state has a higher degree of covalency. It is gratifying to note that the ionicity of the orbitals expressed by the B-values shows the order expected from simple geometrical considerations.

5.2. Octahedral V^{3+}

To explain the absorption responsible for the reddish colour in the untreated crystals grown from a V$_2$O$_5$ flux, the following possibilities will be considered: V^{3+} on octahedral sites, V^{3+} on tetrahedral sites and V^{4+} on octahedral sites. Optical absorption due to V^{3+} on tetrahedral sites should occur at energies lower than observed for V^{4+} on tetrahedral sites. V^{4+} on octahedral sites is expected to produce ESR signals at 4.2 K or even higher temperatures, considering the normally observed trigonal-field splittings. F-state ions like V^{3+} (3d^2) in distorted octahedral symmetry do not produce ESR signals under ordinary experimental conditions (Wertz and Bolton 1972). The ^{3}T$_1$ state, which is the ground state in octahedral fields, is split by the axial field into a doublet and a singlet. Strong spin–orbit coupling between these states leads to a large zero-field splitting and a fast spin–lattice relaxation. Thus the $M_s = \pm 1$ levels are removed too far from the $M_s = 0$ state to permit observation of $\Delta M_s = 1$ transitions. Double quantum transitions may be observed, but fast spin–lattice relaxation makes it necessary to perform ESR measurements at 4 K or lower. Experimentally in the untreated crystals an optical absorption was observed in the region expected for V^{3+} on octahedral sites (compare with table 3), while ESR signals are absent. Therefore both V^{4+} on octahedral sites and tetrahedrally coordinated V^{3+} can be ruled out. An energy level diagram for the 3d^2 configuration of V^{3+} in octahedral sites is shown in figure 4 (Sugano *et al* 1970). The proposed assignments and calculated crystal-field parameters are given in table 6.

Table 6. Optical data, assignments and crystal-field parameters of V^{3+} in octahedral sites.

Transition energy (10^3 cm^{-1})	Assignment	Crystal-field parameter, 10 Dq (cm^{-1})	Racah parameters, B (cm^{-1})
14	^{3}T$_1 \rightarrow {}^3$T$_2$	15700	640
22	^{3}T$_1 \rightarrow {}^3$T$_1$		

In YAG: V^{3+} the corresponding transitions are found at 15800 and 23000 cm^{-1}, in accordance with the smaller value of the lattice constant in YAG ($a_0 = 12.000$ Å; (Euler and Bruce 1965).

6. Discussion

The compositions of the flux-grown crystals and the polycrystalline material differ considerably in the occupation of the octahedral and dodecahedral sublattices. To obtain the figures stated in table 1 the composition of the polycrystalline material has been

assumed to correspond to the weighed stoichiometric fractions, which seems realistic in view of the low temperature of synthesis. This assumption is supported by the good correlation between the different experimental results. The calculated x-ray densities of the single crystals, using the compositions and lattice parameters determined, agree well with the measured values. The total cationic charge is equal to 24 within experimental error if the vanadium ions are present in the highest oxidation state. In crystals grown from PbO fluxes, no reduced vanadium centres could be detected. The results of optical absorption measurement and electron microprobe analysis indicate the amount of triply charged vanadium present in crystals grown from V_2O_5 fluxes to be small. Therefore, in agreement with observations made by Ronniger and Mill (1973), it is concluded that in these garnets, as grown, the tetrahedral sublattice is mainly occupied by V^{5+} ions and any surplus of doubly charged ions is compensated by vacancies in the c and a sublattices, i.e. the crystals used for this study have the compositions ${Ca_{2.05}Na_{0.60}Mg_{0.11}\square_{0.24}}[Mg_2](V_{2.99})O_{12}$ and ${Ca_{1.94}Na_{0.91}Pb_{0.10}\square_{0.05}}[Mg_{1.92}\square_{0.08}]$-$(V_{2.99})O_{12}$ respectively.

In contrast to the results obtained in this study, Desvignes *et al* (1981) have reported a large excess of vanadium—0.17–0.27 V per formula unit—to occur in this garnet, when grown from fluxes with similar compositions. To achieve charge balance in that case, a considerable quantity of reduced vanadium centres must be present, leading to optical absorptions in the visible region. Their assignment of bands seen at 18900 and 20000 cm^{-1} to trivalent vanadium at tetrahedral sites is incompatible with the interpretation of spectral data given in the previous sections. If, however, the absorptions are attributed to four-valent vanadium at octahedral sites reasonable agreement is attained.

The centre is then characterised by a cubic splitting of 10 $Dq \simeq 19000$ cm^{-1} and a trigonal splitting of 1000 cm^{-1}. In comparison with YAG the bands are shifted towards lower energy due to the difference in lattice parameter and because in vanadate garnets the octahedral sites are almost regular, the trigonal splitting is small (Dukhovskaya and Mill 1974). However, a large amount of the vanadium content reported by Desvignes *et al* might be due to the calculation procedure, since the total number of cations has been normalised to eight, which is incorrect if a vacancy mechanism occurs.

Some remarks should be made with regard to the difference between the P value of 172×10^{-4} cm^{-1} predicted by equation (4) and the experimentally determined value of 122×10^{-4} cm^{-1}. The Hartree–Fock wavefunctions used by Malli and Fraga (1967) to calculate $\langle r^{-3} \rangle$ are known to yield theoretical values of interaction constants that approximate the measured ones to within $\pm 5\%$ for the free ions. The discrepancy observed obviously exceeds these limits and must have a physical origin. Quite probably the reduction of P reflects the extension of the wavefunction in the solid state. The same conclusion may be drawn from the results of a more complete description of V^{4+} centres in this and other garnets by Veltrusky (1978). Although the analysis of Veltrusky was complicated by the fact that a number of additional MO coefficients had to be evaluated from the same experimental spin Hamiltonian parameters, and optical data were not available in many cases, a consistent set of ion parameters like λ, κ etc was calculated using an iterative procedure. In his treatment the radial integral $\langle r^{-3} \rangle$ and the spin–orbit coupling constant were used as adjustable variables. The best fit was obtained using a spin–orbit coupling constant only slightly different from the free-ion value and a value of $\langle r^{-3} \rangle$ of 1.79×10^{-23} cm^{-3}, i.e. $P = 124 \times 10^{-4}$ cm^{-1}, very close to our value.

Two features of the optical absorption spectra have not been discussed so far. These are the strong rise in absorption at $\simeq 25 \times 10^3$ cm^{-1} and the increased absorption in the $(15-25) \times 10^3$ cm^{-1} range that accompanies the double band in the infrared. Because the absorption edge is present in samples without V^{4+} centres it must be attributed to V^{5+} ions. Optical reflection measurements are now being performed in the UV region to determine the nature of this absorption; the results will be discussed in due course. The above-mentioned increased absorption cannot be attributed to crystal-field transitions.

In the partly reduced crystals the tetrahedral sites are occupied by V^{4+} and V^{5+} ions simultaneously. A similar situation occurs in V$_6$O$_{13}$ where two out of three vanadium ions contribute one electron to the 3d band system.

Optical data of this compound have been evaluated from reflectivity measurements (van Hove *et al* 1980). After deconvolution the unstructured absorption of this compound in the $(13-30) \times 10^3$ cm^{-1} region has been interpreted as being composed of several transitions between vanadium sub-bands. A corresponding explanation is thought to be appropriate for the garnets discussed.

Finally it is noted that the stoichiometric melting point, mentioned in the literature (Havlicek *et al* 1971), is contradicted by the thermogravimetric experiments performed.

7. Conclusions

A large concentration of vacancies is possible in the Ca$_2$NaMg$_2$V$_3$O$_{12}$ garnet. At high temperatures a reversible weight loss occurs, which is accompanied by the formation of V^{4+} ions at tetrahedral sites. The optical transitions, interpreted in a crystal-field scheme, can be correlated to the ESR parameters by means of MO theory, if a reduced value of the hyperfine interaction is used. This is given justification by the available literature data.

References

Abragam A and Bleaney B 1970 *Electron Paramagnetic Resonance of Transition Ions* (Oxford: Clarendon) pp 167, 416
De Biasi R S 1980 *J. Phys. C: Solid State Phys.* **13** 6235
Desvignes J M, Feldman P and le Gall 1981 *J. Cryst. Growth* **52** 650
Dukhovskaya E L and Mill B V 1974 *Sov. Phys.–Crystallogr.* **19** 47
Durif A 1958 *Proc. Int. Conf. Physics of the Solid State and Applications to Electronics and Telecommunications (Brussels, Belgium)* p 500

Euler F and Bruce J A 1965 *Acta Crystallogr.* **10** 971
Fraga S, Karwowski J and Saxena K M S 1976 *Handbook of Atomic Data* (New York: Elsevier) p 489
Geller S 1967 *Z. Kristallogr.* **125** 1
Gerritsen H J and Lewis H R 1960 *Phys. Rev.* **119** 1010
Havlicek V, Novak P and Vichr M 1971 *Phys. Status Solidi* b **44** K21
van Hove W, Clauws P and Vennik J 1980 *Solid State Commun.* **33** 11
Jain V K and Srinivasan T M 1977 *Z. Naturf.* a **32** 1068
Kivelson D and Neiman R 1961 *J. Chem. Phys.* **35** 149
Kool Th W and Glasbeek M 1979 *Solid State Commun.* **32** 1099
McClure D S 1959 *Electronic Spectra of Molecules and Ions in Crystals* (New York: Academic Press) p 90
Malli G and Fraga S 1967 *Theor. Chim. Acta* **7** 75
Metselaar R 1977 *Interaction of Radiation with Condensed Matter* vol 2 (Vienna: IAEA) p 159
Metselaar R and Larsen P K 1978 *Physics of Magnetic Garnets* ed. A Paoletti (New York: North Holland) p 417
Prokic D 1974 *J. Phys. D: Appl. Phys.* **7** 1873
Rao K V S, Dattatreya Sastry M and Putcha Venkateswarlu 1969 *J. Chem. Phys.* **51** 812
Ronniger G and Mill B V 1973 *Sov. Phys.–Crystallogr.* **18** 187, 339
Ronniger G, Mill B V and Sokolov V I 1974 *Sov. Phys.–Crystallogr.* **19** 219
Siegel I 1964 *Phys. Rev.* **134** A193
Sugano S, Tanabe Y and Kamimura H 1970 *Multiplets of Transition-Metal Ions in Crystals* (New York: Academic Press) p 108
Suryanarayanan R and Krishnan R 1974 *Phys. Status Solidi* a **22** K177
Veltrusky I 1978 *Czech. J. Phys.* B **28** 675
Weber M J and Riseberg L A 1971 *J. Chem. Phys.* **55** 2032
Wertz J E and Bolton J R 1972 *Electron Spin Resonance: Elementary Theory and Practical Applications* (New York: McGraw-Hill) pp 277, 287, 329